PROTEINS
STRUCTURE ■ FUNCTION ■ BIOINFORMATICS

New insights of membrane environment effects on MscL channel mechanics from theoretical approaches

Gaëlle Debret,[1] Hélène Valadié,[1] Andreas Maximilian Stadler,[2] and Catherine Etchebest[1]*

[1] EBGM, INSERM UMR-S 726, Université Paris Diderot, 2 Place Jussieu, Case 7113, 75251 Paris cedex 05, France

[2] Institut Laue-Langevin, BP 156, 38042 Grenoble Cedex 09, France

ABSTRACT

The prokaryotic mechanosensitive channel of large conductance (MscL) is a remarkable integral membrane protein. During hypo-osmotic shock, it responses to membrane tension through large conformational changes, that lead to an open state of the pore. The structure of the channel from Mycobacterium tuberculosis has been resolved in the closed state. Numerous experiments have attempted to trap the channel in its open state but they did not succeed in obtaining a structure. A gating mechanism has been proposed based on different experimental data but there is no experimental technique available to follow this process in atomic details. In addition, it has been shown that a decrease of the lipid bilayer thickness lowered MscL activation energy and stabilized a structurally distinct closed channel intermediate. Here, we use atomistic molecular dynamics simulations to investigate the effect of the lipid bilayer thinning on our model of the structure of the Escherichia coli. We thoroughly analyze simulations of the channel embedded in two pre-equilibrated membranes differing by their hydrophobic tail length (DMPE and POPE). The MscL structure remains stable in POPE, whereas a distinct structural state is obtained in DMPE in response to hydrophobic mismatch. This latter is obtained by tilts and kinks of the transmembrane helices, leading to a widening and a diminution of the channel height. Part of these motions is guided by a competition between solvent and lipids for the interaction with the periplasmic loops. We finally conduct a principal component analysis of the simulation and compare anharmonic motions with harmonic ones, previously obtained from a coarse-grained normal mode analysis performed on the same structural model. Significant similarities exist between low-frequency harmonic motions and those observed with essential dynamics in DMPE. In summary, change in membrane thickness permits to accelerate the conformational changes involved in the mechanics of the E. coli channel, providing a closed structural intermediate en route to the open state. These results give clues for better understanding why the channel activation energy is lowered in a thinner membrane.

Proteins 2008; 71:1183–1196.

Key words: mechanosensitivity; model membrane; hydrophobic mismatch; molecular dynamics; essential dynamics; normal mode analysis; membrane protein.

INTRODUCTION

Mechanosensitive (MS) channels are integral membrane proteins. In prokaryotic organisms they act as true "safety valves" preventing cells from lysis during hypo-osmotic shock. In eukaryotic organisms, they play a role in different biological functions such as hearing, touch, or cardiovascular regulation. For the accomplishment of their function, MS channels are endowed of remarkable mechanical properties: they are able to largely open in response to a mechanical strain that arises in their membrane environment. The formed pore lets pass without ionic selectivity small solutes such as water or ions but also much larger entities such as small proteins such as thioredoxine,[1] even if it does not flux as a globular protein.[2]

The best characterized member of this family is a prokaryotic large conductance mechanosensitive channel (MscL), which was originally isolated from *Escherichia coli* (Eco-MscL) by Kung and coworkers.[3] Since then, numerous electrophysiological and mutational experiments have been performed on the channel.[4–25] These studies led to identify that the fully open state of the MscL consists of a large nonspecific pore with an esti-

The Supplementary Material referred to in this article can be found online at http://www.interscience.wiley.com/jpages/0887-3585/suppmat
Grant sponsor: Action Concertée Incitative "Dynamique et Réactivité des Assemblages Biologiques" (ACI-DRAB, 2003–2006).
*Correspondence to: Catherine Etchebest, EBGM, INSERM UMR-S 726, Université Paris Diderot, 2 Place Jussieu, Case 7113, 75251 Paris cedex 05, France.
E-mail: catherine.etchebest@ebgm.jussieu.fr
Received 27 April 2007; Revised 27 July 2007; Accepted 24 August 2007
Published online 14 November 2007 in Wiley InterScience (www.interscience.wiley.com). DOI: 10.1002/prot.21810

mated diameter of about 40 Å.[6] However, until now, no 3D structure of the open state or of the closed one for *E. coli* has been determined.

Chang *et al.* working on the homologous sequence from *Mycobacterium tuberculosis* (Tb-MscL) succeeded in isolating, purifying, and finally solving the structure of this homologous channel in its closed state by X-ray crystallography[26] (PDB code 1msl). A refined structure (PDB code 2oar) has recently replaced the previous one.[27] It showed that the channel consists of five identical subunits arranged around a central pore. Depending on the localization with respect to the environment, each subunit, predominantly α-helical, can be subdivided into different regions: a transmembrane region, a periplasmic, and a cytoplasmic region. The transmembrane region consists of two helices (TM1 and TM2) connected by a large periplasmic loop. TM helices are tilted of about 30°–35° with respect to the membrane normal. The TM1 helices define the pore, whereas TM2 helices are placed outside of the channel, in contact with the lipids. On the cytoplasmic side, the channel is constricted with a diameter of about 2 Å. This constriction is lined by a cluster of hydrophobic residues (Val-21 for *M. tuberculosis*), which probably constitutes a true gate for the permeation of ions and water molecules.[26]

The large difference observed in the pore diameter between the closed and the open states[20,28] makes it clear that major conformational changes accompany the transition between these two states. Several models of gating mechanism have been proposed. The most studied and the more consistent with experimental data is the one proposed by Sukharev *et al.* and Guy and coworkers.[29,30] This model involves mainly the TM1 helices that would twist and tilt, while TM2 helices would only tilt. Beside this well-accepted mechanism, Sukharev's group proposed a two-step process with different subconductance substates. In this opening model, two gates are involved: the first one corresponds to the Val-23 constriction (in *E. coli*, corresponding to the Val-21 one in *M. tuberculosis*), and the second one is located in the early N-terminal region, defined by the first 12 residues unresolved in the first crystal structure. This domain would fold into α-helix as in the current crystal structure, and the five helices would associate to form a bundle called S1. In the early stage of the gating mechanism, the channel undergoes a conformational transition implying a widening of the transmembrane domain of the pore. In this state, the pore is still occluded by a ring formed by the amino acid side-chains of the S1 helix-bundle. Different experimental data support this mechanism,[30] but surprisingly the recent crystal structure shows that the N-terminal helices do not arrange to form a bundle but are parallel to the membrane plane.[27] Although this model reveals much in regard to the properties of the channel, some questions are still unanswered and there is no experimental technique available to follow the process of pore gating in atomic details.

At a theoretical point of view, many attempts have been done for a better understanding at an atomic scale, the role of each domain and the way they move during the channel gating. Different computations have been performed using mainly molecular dynamics (MD) simulations. Even if extremely useful, these simulations are confronted with the problem of the time scale simulated (few ns) far from the biological one (ms). Consequently, it generally prevents large conformational changes to be observed but provides first insights in the earliest stages of the mechanism.[31] Different strategies may however compensate such limitations and accelerate the motions, that is by working at high temperatures, imposing some constraints as in steered MD, biasing the potential energy as in umbrella sampling. In this context, MD simulations of the *M. tuberculosis* MscL or of the *E. coli* model from Sukharev were performed using different protocols to accelerate the gating conformational changes. Different simulations took advantage of the mechanical feature of the channel, that is its opening under mechanical stress provided by membrane tension and/or membrane curvature.[32–36] The main results obtained by these simulations tended to confirm the general features of the gating mechanism. However, the nature of the constraints and the way they are imposed strongly influence the response of the system, limiting further discussion.

An interesting work has however been realized,[37] based on the fact that decreasing bilayer thickness lowers MscL activation energy, stabilizing a structurally distinct closed channel intermediate.[38] These simulations provided first hints about how the channel may adjust to membrane thinning. However, the changes in membrane thickness were accomplished during the simulations. Such a protocol could influence the way the channel adapts to the membrane thickness change. The authors admitted that the results were obtained under unrealistic conditions and that the methods employed could undergo further optimization.

Moreover, most of the simulations have been conducted on the first crystal structure, that is for Tb-MscL, while most experimental studies are performed on the Eco-MscL. Several differences however exist between Tb and Eco-MscL such as sequence composition, loop length or more importantly, mechanical sensitivity. Indeed, the gating threshold of Tb-MscL is approximately twice as high than that of Eco-MscL.[10,39]

In a previous work,[40] we constructed a homology model structure of Eco-MscL from the X-ray structure of Tb-MscL. We already mentioned that our model differs from that of Sukharev by several aspects: the length of the TM helices, shorter in our model and closer to Tb-MscL length, the tilt of the TM helices, and the location of the periplasmic loops that plunge in the pore as for Tb-MscL. Using a simplified normal mode analysis,[41,42]

we showed that the movement associated to the first lowest normal modes is clearly an "iris-like" movement involving both tilt and twist rotation. Interestingly, these results were obtained without any membrane environment. The similarity of the motions observed in this study with those suggested by Sukharev's group led us to propose that the way the channel opens in response to a mechanical stress, comes from the shape of the channel itself.

The crude representation of the molecule (Cα were only considered) prevented detailed discussion about the precise role of each amino acid. The putative influence of the membrane on the harmonic modes, namely the directions of motions and the regions involved, were not either considered. In addition, anharmonic motions that are discarded by nature in normal mode analysis can contribute significantly to conformational changes of the channel.

Essential dynamics is a good compromise between coarse-grained normal mode analysis and classical MD simulations. Likewise classical MD simulations, it is based on an all-atom description, including the environment and considering anharmonic motions. This approach also permits to filter trajectories from noisy motions, and to extract long time scale and correlated ones as in normal mode analysis. To be efficient and meaningful, this method needs a good sampling of the conformational space, that is long trajectories simulations or numerous different simulations. Nowadays, calculation capability permits to reach simulation times relevant for exploring interesting regions of the conformational space. This approach thus provides information about preferred dynamics directions and conformations.[43–46]

In this work, we address two questions: the role of the environment on the *E. coli* channel conformation and the impact of anharmonic motions. For this purpose, we perform a similar study to the experimental work performed by Perozo *et al.*[38] that consisted in exploring the influence of membrane thickness on the channel structure. Compared to the work of Elmore and Dougherty[37] we consider *E. coli* sequence rather than *M. tuberculosis*, and we truly consider the behavior of the channel placed in equilibrated membranes of different composition.

The inner membrane of *E. coli* cells is mainly composed of lipids with phosphatidyl ethanolamine (PE) headgroup.[47] Thus, we consider this type of lipids in our study. Two model systems were thus explored, both including PE head groups but differing by the acyl chain length, namely POPE (C16:0-C18:1-PE) and DMPE (C14:0-PE), the shortening of the acyl chains length resulting in the decrease of the membrane thickness. Similarly to what was done experimentally, we explore the influence of this parameter on the dynamical and structural behavior of Eco-MscL.

The article is organized as follows: first, we report MD simulations of equilibrated systems of hydrated pure membranes of DMPE and POPE. Then, we investigated thoroughly the behavior of the channel model (close to Tb-MscL structure) embedded in both environments. Numerous simulations with different protocols were performed to get a large sampling. We finally compare harmonic and anharmonic motions through the projections of the principal components of the molecular dynamic simulations on the low-frequency normal modes.

MATERIALS AND METHODS

Membrane construction

The two types of lipids investigated are, respectively, POPE, that is C16:0-C18:1-PE and DMPE, that is C14:0-PE.

We first simulated pure equilibrated membranes. For POPE, we started from a pre-equilibrated membrane with 340 lipids and 6729 water molecules, kindly provided by Tieleman (http://moose.bio.ucalgary.ca/index.php?page=Structures_and_Topologies).[48] The system was enlarged in the *z* direction to adapt to the channel size.

For DMPE, no parameter and no pre-equilibrated system were available. Therefore, we first constructed the lipid itself from a combination of a 1,2-dimyristoyl-sn-glycero-3-phosphocholine lipid (DMPC) for the acyl chain and POPE for the headgroup. A pre-equilibrated system (kindly provided by Tieleman) consisting of 128 DMPC and 3655 water molecules was used as a basic structure. The headgroups of the DMPC molecules were removed and replaced by phosphoethanolamine such as bond lengths and steric constraints were respected. This system was used as a starting structure. After energy minimization and 1 ns simulation at 300 K, the system was stable. To take into account the different phase transition temperatures from gel to liquid-crystalline of the two lipid membranes, we continued the simulations for 1 ns for DMPE, slightly increasing the temperature to 330 K. As a control, a simulation at 300 K for 1 ns was done in parallel for DMPE, POPE, and DMPC. One simulation for the DMPE membrane system at 330 K and one for the POPE membrane system at 300 K were extended for 5 ns. The simulations were performed using Berendsen isotropic pressure coupling. Because of the size of the system examined, we chose cut-off approximation for long-range electrostatics contribution. We selected large values, that is 18 Å cutoff. These conditions have been verified with two additional 2-ns simulations in DMPE: the first one with semi-isotropic pressure coupling, the second one with PME electrostatics calculation.

At the end of the simulations, we selected equilibrated molecules contained in a box with dimensions 45, 45, and 66 Å. This subset corresponded to 68 lipids and 2045 water molecules. The system was minimized and finally duplicated to yield a system containing 272 lipid

Table I
Performed Simulations Characteristics

Lipid type	Electrostatics treatment	Pressure	Temperature (K)	No.	Time (ns)	Constraints
POPE	Cut-off	Isotropic	300	3	5.0	
	Reaction-field	Semi-isotropic		1	5.0	
DMPE	Cut-off	Isotropic	330	3	4.0	
				1	5.0	4 N-terminal residues position
				1	10.0	$i - i + 4$, distance in TM helices
				1	2.0/5.0	Protein backbone for 2 ns then relax
			300	2	4.0	
			300/330*	1	4.5	
	Reaction-field	Semi-isotropic	330	1	5.0	

*300 K for protein and 330 K for lipids.

molecules and 19,191 water molecules, and corresponding to a box of 90, 90, and 106 Å.

Insertion of the MscL in membrane systems

Mutational studies on MscL of *E. coli* showed that a deletion starting at residue 110 does not modify the behavior of the protein.[49] To conserve a functional system and to reduce the number of atoms, every monomer of the Eco-MscL protein was truncated after residue 110. The RKKxE motif was conserved.[23] To neutralize the system, five counter-ions (Cl^-) were added. The truncated channel was fully solvated and simulated for 1 ns at 300 K, with strong constraints on the polypeptide backbone of the TM1s and on the entire loops and TM2s. Thus, only side-chains of TM1 and water molecules were free. At the end of the simulation, only water molecules in the pore and in contact with loops were kept. This procedure permitted to obtain an equilibrated structure of the pore interior solvated in a short time. The solvated structure of the channel was then placed in the membrane (POPE or DMPE) so that residues Leu86 and Ile87 were in the centre of the lipid bilayer.[13] Lipids superimposed on the channel and lipids with bad contacts were removed. The systems containing the channel, the lipids, and the pore waters were then solvated and minimized. POPE Eco-MscL system contained 260 lipid molecules and 18,408 water molecules, whereas DMPE Eco-MscL included 180 lipid molecules and 16,350 water molecules Finally, POPE and DMPE systems represent, respectively, 73,434 and of 62,020 atoms. For each system, we first performed a short simulation (250 ps) constraining the protein and letting lipid and water molecules to adapt to the channel.

MscL in membrane simulations

We performed three 5 ns simulations in POPE at 300 K and three 4 ns simulations in DMPE at 330 K differing by the initial velocities, with cut-off electrostatic treatment and constant pressure using the Berendsen algorithm. Various temperatures were used for the systems with POPE and DMPE membranes because of the different phase transition temperatures. The detailed analyses described in this article were performed on these simulations. We also carried out additional simulations to test the influence of different parameters such as temperature, pressure coupling, constraints, and electrostatics treatment (Table I). For all these simulations, we checked that the main effect of the membrane change on the MscL channel structure was similar.

Simulation details

All the minimizations and MD simulations were performed with GROMACS 3.2.[50,51] Lipid parameters were taken from Berger *et al.*[52] Gromacs force field parameters (ffgmx) were used for protein and the SPC water model. All bonds were constrained with the LINCS algorithm,[53] thus permitting to increase the integration time step to 2fs. The SHAKE algorithm[51] instead of LINCS was used to constrain the bonds when distance restraints were applied. Structures from trajectories were saved every picoseconds. Isotropic pressure coupling was used with a coupling constant of 0.1 ps. Temperature was coupled separately for protein, lipids, solvent, and ions with a coupling constant of 0.1 ps[54]; for electrostatics, a twin range cut-off equal to 1.8 nm was used and 1.0 nm for vdw interactions. Semi-isotropic ensemble was used with RF (rvdw equivalent to 1.0 nm and rcoulomb to 1.8 nm) method simulations.

Most of the analyses were performed with Gromacs tools. The different domains of the protein were defined as residues 21–40 for TM1, 41–76 for the periplasmic loop, and 77–97 for TM2. Some additional tools were developed in C language and are available upon request to the authors.

Pore diameter calculation has been realized with HOLE[55] and visualization with the VMD program.[56] NMA results have been taken from a previous study.[40]

Geometrical analysis

Different parameters specific to the MscL dynamics were analyzed, as tilts and kinks of the transmembrane helices.

The tilt angle is defined as the angle between the membrane normal and the axis of inertia of the considered TM helix. To relate tilt and membrane thickness more easily, we have also considered the projection value of the length of the TM axis on the membrane normal. This distance called the height of the helix in the text is computed between two residues, corresponding to the extremities of the TM, V21 and I40 for TM1, and V77 and K97 for TM2. We also considered the position of the loops (residues 41–76) with respect to the membrane and defined similarly, a loop height. The height of the loop is the distance between the centre of mass of the loop and the centre of mass of the cytoplasmic ends of TM1 and TM2 (residues V21 and K97). Finally, we defined the membrane thickness as the projection on the membrane normal of the vector joining the center of mass of the P atoms of each lipid leaflet.

For the kink angle, each residue of the helix is tested as a potential pivot and the angle between axes of inertia of the subhelices on each side of the pivot is calculated. The maximum angle value and the associated pivot are kept as the kink angle value and the hinge residue.

PCA analysis

Principal component analysis was performed with Gromacs tools on concatenated trajectories [15 ns (15,000 frames) for POPE and 12 ns (12,000 frames) for DMPE, respectively]. We checked that the cosine content of eigenvectors is different from 1 and thus that the described motions are not related to random diffusion.[57] Therefore, all the obtained principal directions clearly describe relevant conformational changes.

Overlap calculation

The overlap measure I quantifies the degree of similarity between two directions defined by vectors a and b, respectively. We chose the definition proposed by Marques and Sanejouand[58]:

$$I = \frac{\left|\sum_{i=1}^{3N} a_i b_i\right|}{\sqrt{\sum_{i=1}^{3N} a_i^2 \sum_{i=1}^{3N} b_i^2}} \qquad (1)$$

Overlap values were computed between each principal vector and each normal mode. The similarity of the principal eigenvectors describing the trajectories in each environment was also computed.

Participation

Contribution of each eigenvector to the fluctuations observed in each system is defined as the overlap between the considered eigenvector and the vector linking the initial conformation and a given final conformation. This latter is defined as the average conformation over the last structure of each included simulation superposed with the program Profit. Participation is expressed as a rate, that is 100% representing identical directions.

Collectivity

The collectivity κ measures the collective protein motions within a given mode or eigenvector (i.e. the number of atoms significantly affected). It has been calculated as described by Bruschweiler[59]:

$$\kappa = \frac{1}{N}\exp\left(-\sum_{i=1}^{N} \alpha A_i^2 \log \alpha A_i^2\right) \qquad (2)$$

where A_i is the amplitude of displacement and α is a normalization factor such as $\Sigma\alpha A_i^2 = 1$. The conformational change is maximal for a value of 1 and minimal for a value of $\frac{1}{N}$.

RESULTS

Pure membrane simulations

Exploration of lipids influence on the protein behavior first requires reliable membrane systems. Pure solvated DMPE and POPE bilayers were thus simulated and different parameters were checked before embedding the channel into them. Facing the problem of the sparse experimental data available for DMPE system, one additional simulation was performed on pure solvated DMPC membrane to assess the simulation conditions. Different parameters were carefully examined, but we focused mainly on the hydrophobic membrane thickness (supplementary data s1). The results showed that after an equilibration period, it remains stable all along the simulations. The difference between the two PE systems is roughly equal to 8 Å, POPE being larger than DMPE (and DMPC).

Overall, the results are consistent with the experimental data available.[60–62]

Stability of the MscL in POPE

MscL protein lacking the C-terminal domain was placed in the equilibrated POPE membrane selected at the end of the production step. Details of the procedure are given in Materials and Methods section. The placement of the protein along the membrane axis, initially defined by the position of two residues Leu86 and Ile87, remained extremely stable all along the simulations. The behavior of the different domains (TM1, TM2, periplasmic loop, N and C extremities) of the protein was carefully followed in all the different simulations [Fig. 1(a,b)]. The contacts existing at the beginning of each simulation between the lipid polar headgroups and the

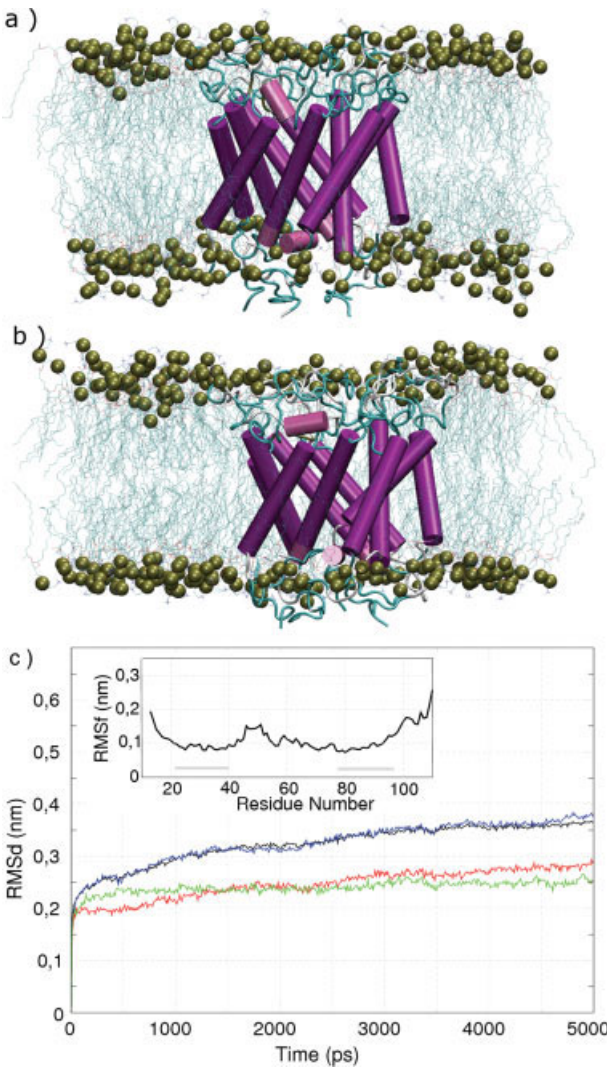

Figure 1

*MscL in POPE membrane: (**a**) Starting conformation at t=0ps and (**b**) a representative conformation extracted at the end of a trajectory at t = 5ns. For the POPE membrane, only Phosphorous atoms are represented as 'Van der Waals' spheres, MscL is represented in cartoon with VMD software and colored according to secondary structures (α-helices are in purple and loop regions in light cyan). (**c**) Mean Cα RMSd for the entire protein (black), for the TM1 helices (red), for the TM2 helices (green) and for the periplasmic loops (blue). The inset represents the Cα RMSf along the sequence. Transmembrane helices are indicated with a gray line. Averages are computed over the five subunits and considering all the simulations. [Color figure can be viewed in the online issue, which is available at www.interscience.wiley.com.]*

PL loops, as well as with the N- and C-terminal extremities, hold all along the trajectory. The transmembrane regions do not exhibit any significant rearrangement. All these features confirm an appropriate placement of the protein with respect to the membrane and the solvent. The main results being quite similar for all the simulations, only averages and standard deviations for the relevant examined parameters are reported.

The Eco-MscL model structure remains relatively stable during the time course of the simulations as illustrated by the RMSD plot of the Cα atoms [Fig. 1(c)]. After 3.5 ns, Cα RMSD reaches a plateau of 3.8 Å. Each region of the protein contributes differently to this value: as expected, loop regions are responsible for the larger part of the deviation (3.5 Å), while TM2 and TM1 transmembrane helices deviate by only 2.5 Å from the starting conformation. Such RMSD values were already observed for MscL of *M. tuberculosis*[33,63] and other membrane protein simulations,[64,65] in a membrane environment, using different force fields and/or molecular dynamic programs. In addition, whatever the considered simulation, these values are rather stable.

Analysis of the secondary structure along the simulations (supplementary data s1) confirms the stability of the TM regions, which mainly remain α-helical. Overall, the protein structural model is stable in the POPE environment, whatever the simulation, providing strong evidence of its relevance.

Conformational changes of the MscL in DMPE

In DMPE, the channel was placed according to the same protocol (see above and Materials and Methods section). In any simulation, the two reference residues, Leu86 and Ile87, remain at the interface between the acyl ends of the two leaflets, providing supplementary evidence of the stability of the model [Fig. 2(b)]. A very large number of simulations were also performed to evaluate the putative influence of the simulation conditions on the results, yielding a total of more than 40 ns. Even if differences exist between all the simulations, the behavior of the system is quite similar. Average values and standard deviations are therefore described here.

Significant structural rearrangements are observed as indicated by the large values of the Cα RMSD (twice the value in POPE) [Fig. 2(c)]. After a large and rapid increase in the first picoseconds of the simulations, the Cα RMSD reach a plateau at 6 Å. Analysis of the contribution of each domain (TM1, TM2, and periplasmic loops) confirms significant differences with POPE simulations, especially for TM1 and TM2 helices. Loop deviation is about 5.5 Å; while TM1 and TM2 deviations are about 4.0 Å. Fluctuation profiles along the sequence are similar to the POPE fluctuations profile, even if the values are larger [see inset of Figs 1(c) and 2(c)]. These large rearrangements clearly originate from the change in membrane thickness. It leads the various regions of the protein to experience different physico–chemical environments. For instance, at the beginning of each simulation, the loops and the N- and C-terminal ends are in contact with the solvent. Likewise, even if the transmembrane helices are mainly located in the hydrophobic part of the membrane, the TM ends are in contact with the polar head-

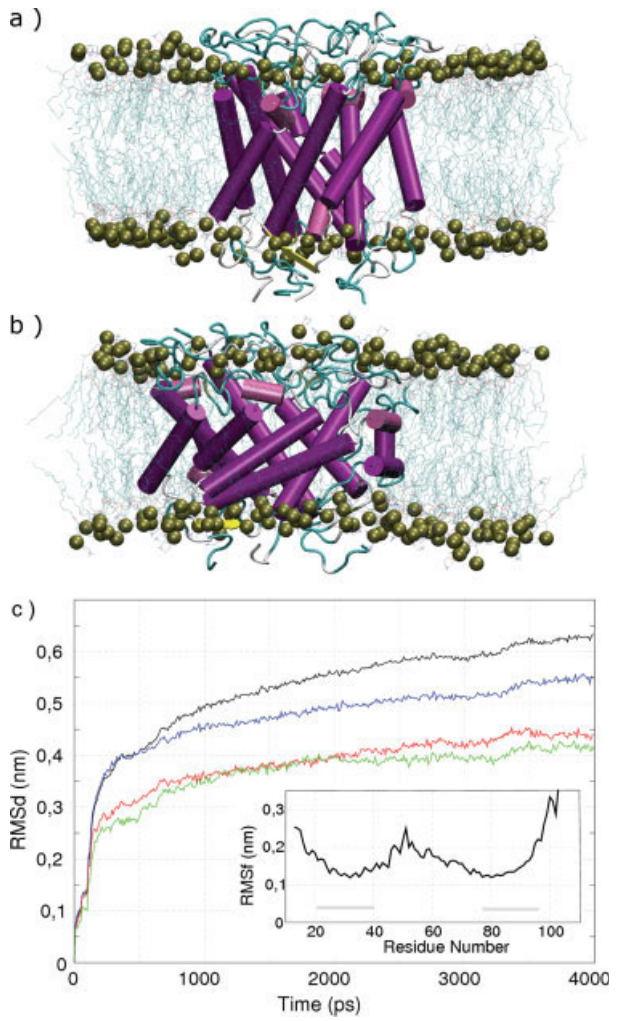

Figure 2

Same as Figure 1 for simulations in DMPE. End of the trajectory corresponds to 4ns. [Color figure can be viewed in the online issue, which is available at www.interscience.wiley.com.]

groups. Progressively along each simulation, loops escape from the polar solvent medium to finally make contacts with the lipid headgroups, as in the starting conformation in POPE. TM helices (mainly TM1) move to diminish contacts with the polar solvent. Interestingly and more importantly, these large conformational changes still preserve the helical secondary structure (see supplementary data s2), except in the central region of most TM1. There, the hydrogen bond network is perturbed, which is concomitant with the formation of a kink.

MscL helices tilt in reaction to hydrophobic mismatch

Different geometrical characteristics of the channel were analyzed to better understand the nature of the conformational modifications, consecutive to the membrane thinning. The tilt angle is one of the major characteristics of the transmembrane helices in a membrane helix bundle. It is also known to be related to the membrane thickness.[66] Indeed, it largely increases from 35° to 50° for TM1 and from 35° to 45° for TM2 in DMPE, whereas it remains stable in POPE. We chose to describe in more details distance measures (height) to compare the changes in helix positioning with the membrane thickness (see Materials and Methods section).

In POPE [Fig. 3(a)], the height of the TMs and the loops is stable. Similarly, the membrane thickness (~41 Å) is maintained all along the simulation even if some difference between bulk and contacting POPE lipids can be observed. A possible explanation might be the increase of the favorable interactions between lipids polar head groups with the periplasmic loops (see Energetic contributions section). In this case, the energetic balance between conformational changes in the loops and the

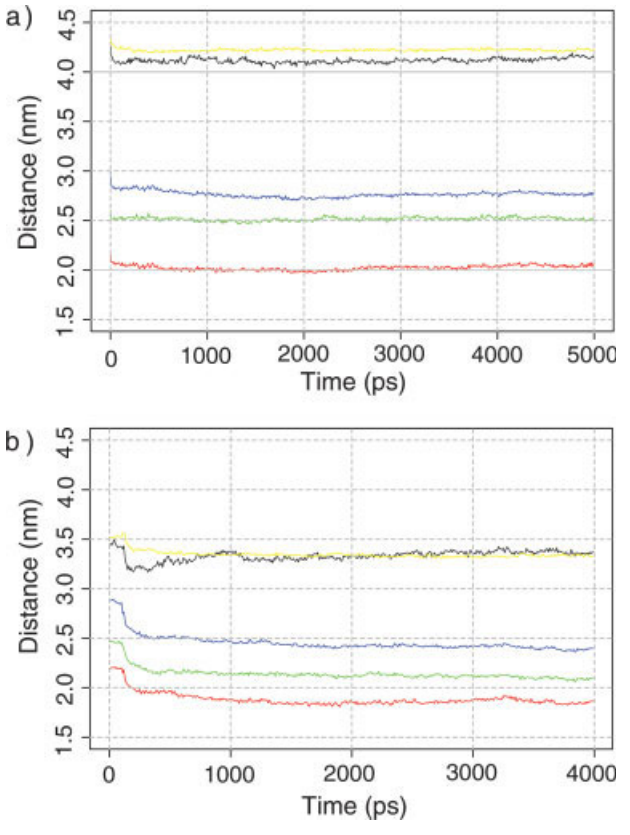

Figure 3

*Mean height of the different regions of the proteins during the simulations (**a**) in POPE, (**b**) in DMPE, with TM1 in red, TM2 in green, periplasmic loops in blue. Membrane thickness (P–P distance) is represented in black for lipids in contact with the channel and in yellow for lipids in the bulk phase. Mean is computed from the five subunits and considering all the simulations at the time considered.*

rearrangement of the contacting lipids seems to favor a slight invagination in the lipids.

In contrast, in DMPE [Fig. 3(b)], the height of the TMs and the loops decreases abruptly of about, respectively, 3 Å and 4.5 Å during the first hundreds picoseconds. Then, the values equilibrate. Even if the tilt of the helices results in changes in the loops height, it is also due to self-conformational changes. Indeed, the loops tend to plunge more deeply inside the channel vestibule. In comparison, membrane thickness remains relatively stable, close to the channel pore as in the lipid bulk phase. Interestingly, at the beginning of the simulation, during few hundreds picoseconds, the lipids near the channel tend to adapt to the channel changes, diminishing the distance between the two leaflets. Then, the distance increases again to finally reach the initial value. Afterward until the end of each simulation, bulk and contacting lipids height are similar. Contrary to POPE, interactions favor the adaptation of the channel to the hydrophobic mismatch (see Energetic contribution section).

At the end of each simulation, TM helices as well as a large portion of loops are completely buried into the hydrophobic membrane domain. Clearly, Eco-MscL undergoes large rearrangements in a thinner membrane, to maintain optimal interactions with lipid headgroups and to avoid contacts with solvent.

To evaluate any putative artifact consecutive to different equilibrium timescale for the membrane and the protein, or eventual kinetic traps, we performed a simulation where the channel was constrained during a few nanoseconds and the membrane was free to adapt to the channel. During this period, we have observed that the lipids close to the channel got thicker to better cover the hydrophobic domain of the channel, yielding a significant increase of the hydrophobic membrane thickness. However, when the whole system was fully relaxed, the TM helices tilted and the lipids close to the channel went back to their initial positions.

Helix kink

The tilt angles described earlier are obtained considering helices as true cylinders with straight axis. Helices are in fact flexible and deformable. Most deformations are related with local breaks in the H-bond pattern. From this break region, helices can kink with different amplitudes in different directions. In POPE, the mean kink reaches 22° for TM1 and 33° for TM2 while in DMPE the mean value is 31° and 33°, respectively, for TM1 and TM2. This value can even reach 68° for some subunits. In POPE as in DMPE simulations, TM1 helices kink is located in more than 70% of the cases in residue G30. This residue is very flexible and close to a functionally important residue K31.[5,15,16] It can be noted that this flexibility also influences the height of the helices.

Helix azimuthal rotation

In POPE as well as in DMPE, no major break in the hydrogen bond pattern occurs in the TM2 helices even if they are curved. Thus, they remain stable and can be considered as only one rigid body regarding the rotation around the axis. For TM1 helices, breaks in the hydrogen bond network involve a relative independence of rotation of the two subhelices on both sides of the hinge point. Thus, they are considered as two independent blocks.

In POPE [Fig. 4(a)], all the helices rotate of about 10° clockwise in the very first steps and then remain stable until the end of the simulations. This early light rotation change corresponds to an adaptation to the hydrophobic environment. In DMPE [Fig. 4(b)], a progressive 30° clockwise rotation occurs in the first nanosecond for TM2 and Ccap-TM1 helices, whereas Ncap-TM1 only rotates of about 10°. The tilt increase of the helices is associated with a clockwise rotation of both TM1 and TM2 helices.

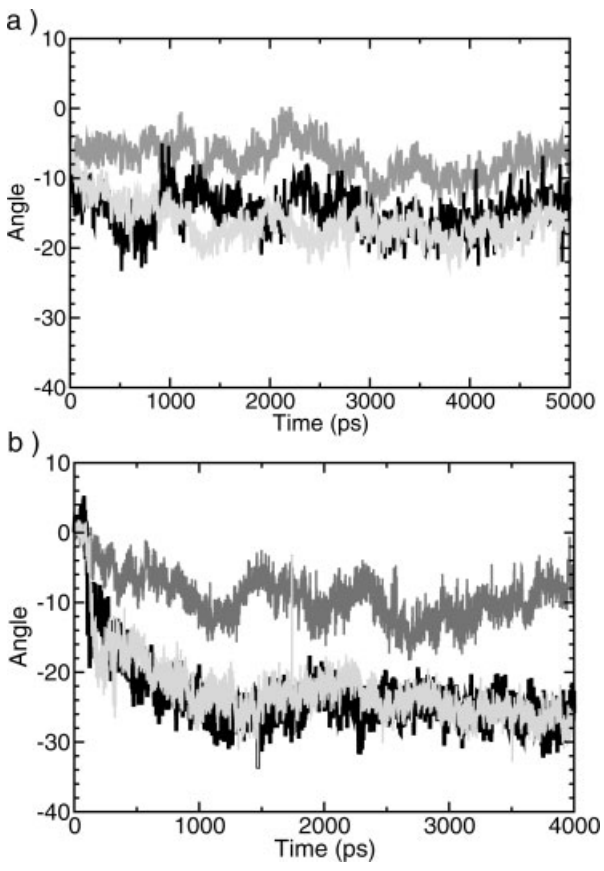

Figure 4

*Mean azimuthal angle as a function of time. Average is computed over monomers and simulations (**a**) for POPE simulations, (**b**) for DMPE simulations. In light gray TM2, in dark gray Ncap-TM1 and in black Ccap-TM1.*

Pore profile and MscL channel radius evolution

Apart the tilting of the TM helices that modifies the height of the channel, additional changes affect the pore shape and its dimensions. For instance, the component of the gyration radius in the plane of the membrane increases in DMPE (12% of the initial radius) whereas it remains stable in POPE. The minimal diameter of the pore is almost not modified during simulations in POPE and the constriction region around V23 is maintained all along the trajectories. As an illustration, pore profiles for different simulations and different time steps are available in supplementary data s3. In DMPE, the pore tends to enlarge and is less constricted in the region close to V23. However, pore shape strongly depends on the side chains conformations, which are long and flexible in MscL. The absence of secondary structure anchors in the cytoplasmic extremities may constitute an artifactual gate in some cases. Thus, a characteristic shape of the pore in the intermediate state obtained is difficult to obtain. However, even if the global diameter of the pore increases, the channel remains close at all time during the time course of the simulations.

Energetic contributions

Interaction energies between the different domains of the protein and between these domains and the environment for both POPE and DMPE are given in supplementary data s4. In POPE, most terms are very stable, in particular the intrinsic contributions that stabilize the channel structure itself. Only the terms related to the interactions between the channel and its environment (POPE-loop and SOL-TM1) are slightly improved. The environment progressively adapts to the channel without perturbing its structure. This confirms the stability of the structure.

Although the conformational changes observed in DMPE, the intrinsic interactions that stabilize the channel are similarly maintained. In particular, the interactions between the transmembrane domains are quite stable. In contrast, larger changes are observed for the interactions between the membrane and the channel along the simulations. Interestingly, interactions between membrane and transmembrane helices or loops are reinforced at the detriment of interactions with the solvent. Despite motions of the TM1 helices and changes in the pore size, the interaction TM1-solvent remains quite constant along the simulations.

Because of the different number of environment molecules in both systems, direct comparison of the different terms is quite difficult. However, in both cases, the conformational energy of the channel is very similar confirming the conformational plasticity of the channel.

Concerted motions with principal component analysis of the trajectories

Principal component analysis permits to highlight high-amplitude concerted motions. The different trajectories in each environment were so analyzed, pooling all together each trajectory. We mainly focused on Cα contribution to understand the motions more easily.

In POPE, the 10 first eigenvectors of the PCA (noted POPE-PCA in the following) contribute to more than 85% of the overall movement; the largest contribution being due to the first eigenvector that accounts for more than 70% of the total motion (see Fig. 5). The following eigenvectors contribute at most to 10% of the overall motion. The motion corresponding to eigenvector 1 involves mainly the N- and C-terminal extremities that are associated to small displacements roughly parallel to the membrane plane (see insets of Fig. 5). The motion also involves the periplasmic loops even if the amplitudes are smaller. TM helices remain very stable. These results illustrate that the MscL does not exhibit large concerted motions on the timescale considered.

In contrast, in DMPE, the overall motions (98%) may be described with four eigenvectors (noted DMPE-PCA below), eigenvectors 1 and 3, respectively, contributing to ~55% in 35% to the motion. The amplitude of movements associated with these two eigenvectors is larger than is POPE (data not shown). In addition, despite some similarities in the motion described by the first eigenvector in POPE and in DMPE (the regions concerned are similar), the type of motion is different. In DMPE, the motion mainly results in a compression of

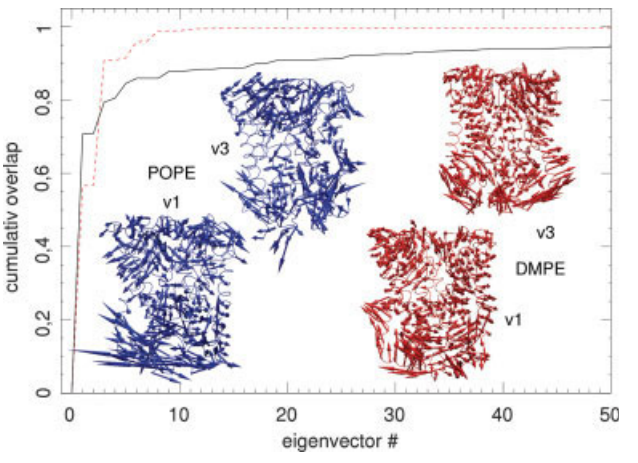

Figure 5

Cumulative PCA eigenvectors participation ratio to the global movement for POPE (full line) and for DMPE (dashed line). Insets represent movements associated to eigenvectors 1 (noted v1) and 3 (noted v3) for both systems. MscL is represented as tube, direction of movements by arrows with length proportional to the amplitude of movement. [Color figure can be viewed in the online issue, which is available at www.interscience.wiley.com.]

the channel. The cytoplasmic ends of the TM helices go up toward the lipid membrane center whereas periplasmic ends go down. Loops tend to hide in the interior of the pore. Eigenvector 3 describes similar movements, the main difference lying in the relative amplitude of each monomer. Global movement in DMPE could then be resumed as a compression of the channel along the membrane axis, accompanied with an enlargement. This motion occurs through the tilting and some kinks of the TM helices.

PCA comparison

As described earlier, lipid bilayer thickness influences the dynamical behavior of the channel. To better characterize the similarities and differences in the concerted motions occurring in each environment, we performed a systematic pair-by-pair projection of the eigenvectors computed in each type of membrane. Large projection values are indicative of similarities in the concerted motions of the channel in both membranes, and could be considered as the intrinsic characteristics of the channel, namely its putative mechanical attributes whatever the channel environment.

The projection values (or overlap) have been computed for the 30 first DMPE-PCA and POPE-PCA eigenvectors. The largest overlap (0.33) is obtained between the DMPE-PCA eigenvector 3 and POPE-PCA eigenvector 4. The movements correspond to the burying of the loops associated with a slight tilt of the TM helices and a displacement of the C-terminal extremities toward the centre of the membrane (see Fig. 6). The collectivity value is 46% and 43% in POPE and DMPE, respectively, namely, roughly half of the atoms are concerned in the specific motions. Even if the movements are slightly noisier in POPE, the global directions are the same as in DMPE. Such movements are thus present in both environments but are amplified in DMPE. Except these two eigenvectors, we did not observe any other significant overlap between eigenvectors deduced from the two sets of simulations. This observation confirms the role of the lipid environment on the MscL dynamics.

PCA and NMA comparison

The final question we addressed concerns the intrinsic mechanical sensitivity of the channel. For that purpose, we compared the results obtained previously with NMA analysis[40] and those obtained from the PCA analysis. A pairwise projection of DMPE-PCA and POPE-PCA eigenvectors with normal mode directions (noted NMA-mode) was thus performed.

For POPE, only two eigenvectors exhibit a significant overlap (larger than 33%) with NMA-modes: NMA-mode 12 with POPE-PCA mode 8 and NMA-mode 15 with POPE-PCA mode 12, with overlap values reaching

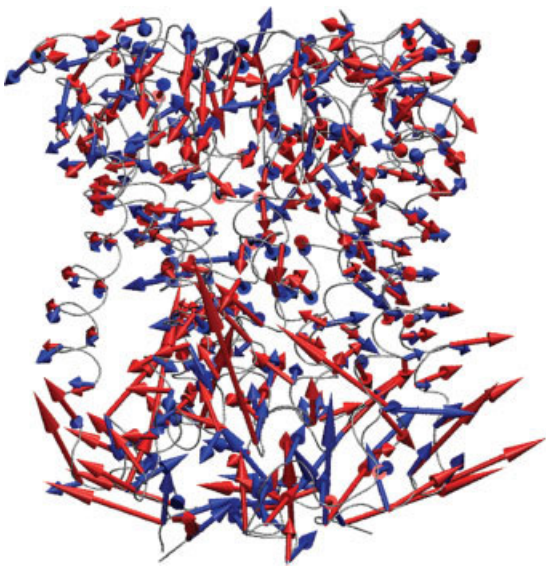

Figure 6

Superposition of motions associated to POPE-PCA eigenvector 4 (blue) and DMPE-PCA eigenvector 3 (red). MscL is represented as tube, direction of movement by arrows with length proportional to the amplitude of movement. [Color figure can be viewed in the online issue, which is available at www.interscience.wiley.com.]

respectively 36.5% and 39.5%. The motions associated with these vectors are represented in Figure 7(a,b). Even if noisier in POPE, the motions are similar and do not correspond to directions that may yield to an open state. This result is in agreement with the mechanical functioning of the channel that requires tension to open.

In comparison, a larger number of DMPE-PCA eigenvectors present significant similarities with NMA-modes. Five overlap values are larger than 33%: DMPE-PCA eigenvectors 1, 3, 10, 17, and 20 with NMA-modes 7, 27, 16, 22, and 13, respectively. The motions associated with the largest overlap (49% between DMPE-PCA eigenvector 3 and NMA mode 27) are presented in Figure 8. These motion corresponds to a compression of the channel (see our previous work[40] for a detailed description). A widening of the TM domain, principally in the cytoplasmic side, is also observed. Collectivity is 43% for DMPE-PCA eigenvector and 49% for NMA mode. Therefore, the adaptation concerns a large part of the structure. In addition, the large overlap between the first mode of NMA (mode 7) and the first DMPE-PCA eigenvector (eigenvector 1) is quite interesting and important. Indeed, it means that the response of the channel to the change of the membrane thickness is not artifactual but is really because of the structure itself. DMPE environment has thus permitted to amplify the intrinsic motions of the channel and has driven it in a state relevant to the channel opening. So, the membrane influences the structure of the channel but does not modify its natural mechani-

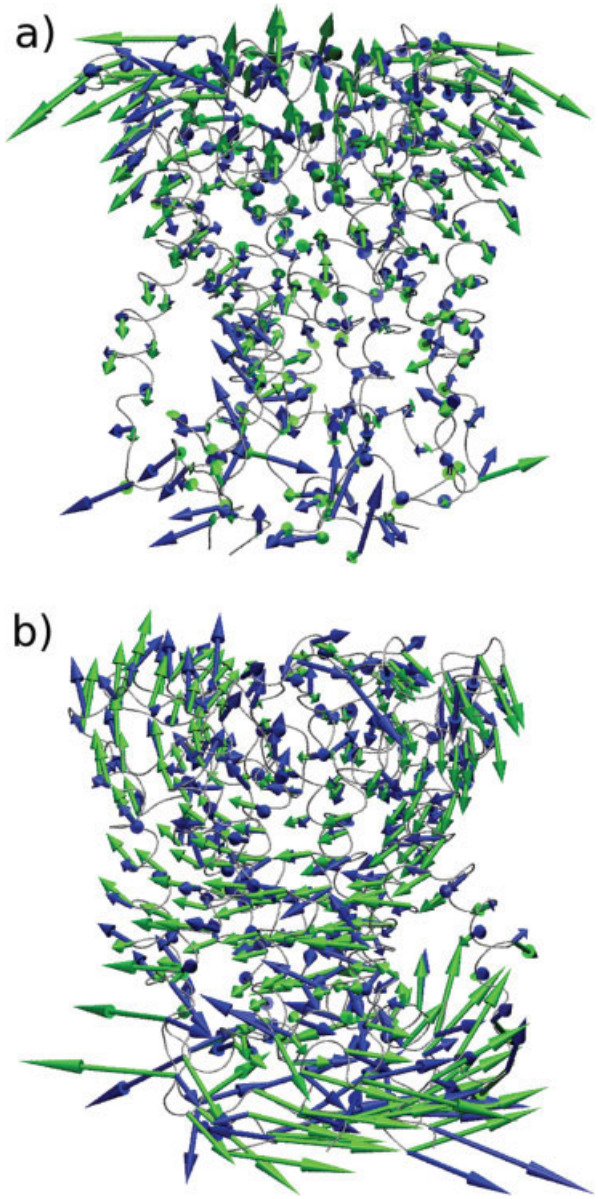

Figure 7

*(**a**) Superposition of motions associated to POPE-PCA eigenvector 18 (blue) and NMA eigenvector 12 (green) respectively. (**b**) Superposition of motions associated to POPE-PCA eigenvector 12 (blue) and NMA eigenvector 15 (green) respectively. MscL is represented as tube, direction of movement by arrows with length proportional to the amplitude of movement. [Color figure can be viewed in the online issue, which is available at www.interscience.wiley.com.]*

cal behavior, that is the directions of motions and the protein parts participating in the motions.

DISCUSSION

The main conclusions we can draw from this study are slightly different from the observations obtained from previous simulations works. We are thus discussing different points that may explain these discrepancies. First of all, the main point that we would like to stress concerns the structural model used.

Importance of the structural model

Most of the previous studies exploring the *E. coli* sequence have focused on Sukharev and Guy's model (SG's model).[34] We have previously discussed[40] the significant differences that exist between this model and ours: the lengths of the α-helices are for instance longer in SG's model, resulting in shorter periplasmic loops. In the closed state, several salt bridges (Lys 55 and Asp 53) between periplasmic loops of different subunits are also present. In the open state, these salt bridges are supposed to be broken. The presence of these salt bridges can increase the barrier for protein conformational changes and on the time scale of the simulations performed, such strong interactions are difficult to disrupt. This is the reason why Gullinsgrud and Schulten[34] had considered alternative conformations for the concerned side chains, privileging intrasubunit salt bridges. In our closed state model, no salt bridge is present in this region. This can explain why conformational changes are facilitated in similar conditions.

The structural model we proposed seems yet valid if one considers its significant stability when simulated in appropriate lipids (POPE). For all the simulations performed, whatever the condition tested, the RMS deviations for the transmembrane regions were quite similar and were in the same range as observed for MD simula-

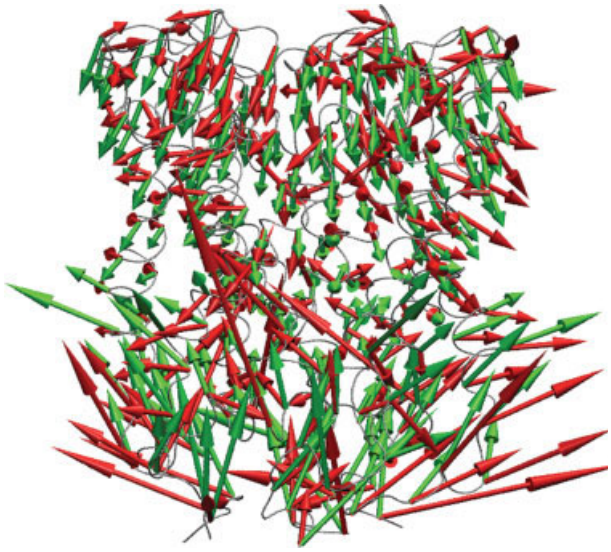

Figure 8

Superposition of movements associated to NMA-mode 27 (green) and DMPE-PCA eigenvector 3 (red). MscL is represented as tube, direction of movement by arrows with length proportional to the amplitude of movement. [Color figure can be viewed in the online issue, which is available at www.interscience.wiley.com.]

tions of different transmembrane proteins[64] using different force fields, different lipids, and different protocols of simulation.

Influence of simulations conditions

We have performed various simulations wherein numerous conditions (initial velocities, temperatures, restraints, and electrostatics) have been changed. In all cases, we observed similar results and the conclusions drawn about the effect of the membrane thickness are quite alike. For instance, by comparing results obtained with cut-off approximation for electrostatics or with the reaction-field treatment, the tilt of the transmembrane helices in DMPE increases compared with the tilt in POPE. The main difference lies in the time taken to reach the equilibrium plateau. Simulations in DMPE were performed at 330 K, compatible with a liquid phase of the membrane. We have performed additional simulations with a lower temperature and still observed the same features.

Influence of the membrane thickness

Elmore and Dougherty[37] already addressed the effects of lipid tail lengths on MscL with MD simulations. Their simulations differed from previous simulations where the transmembrane protein is directly embedded in an equilibrated membrane of chosen thickness. Indeed, they chose to simulate the gradual thinning of the membrane, progressively shortening the lipid tails during the simulations. This procedure was supposed to serve as a crude approximation of the application of tension to the lipid–protein system. In addition, they studied *M. tuberculosis* sequence rather than *E. coli* one and they included the whole cytoplasmic domain. Our study is thus the first one where the influence of the membrane thickness is truly tested for the *E. coli* sequence of MscL channel. The results they obtained showed a clear evidence of hydrophobic mismatch between MscL and the surrounding lipids, that is lipids that directly border the protein thin less than lipids in the bulk of the membrane. Large structural rearrangements were observed but limited to one or two subunits. Conformational changes were also different depending on the simulations. In any case, the Tb-MscL channel seemed to adjust its hydrophobic length with minor changes. This last result is quite different from those we described in this article. Indeed, whatever the simulation in DMPE considered, the channel systematically adapts to the thickness of the membrane with rather large conformational changes, by tilting, kinking, and rotating the transmembrane helices. This may be attributed to different reasons. First, the sequence examined is different. The *E. coli* MscL requires lower tension to open compared with *M. tuberculosis* one. It could mean that conformational changes required for the channel to open are easier to achieve for *E. coli*. Second, we have chosen to simulate the behavior of the protein embedded in an equilibrated membrane composed of different lipids. This study is thus much more similar to the experimental study conducted by Perozo *et al.*,[38] where they examined the conformational changes of the *E. coli* MscL in membranes with different thickness. The study we performed here provides details about the proposed intermediate state where transmembrane helices are tilted and kinked. In addition, we stress a point, frequently discarded, that concerns the significant role played by the periplasmic loops in accompanying the conformational changes. Experimentally, the few data available[12,17] led to the proposal that the periplasmic loop functions as a spring resisting the movement of the transmembrane helices. Our study shows clearly that a part of the observed motions is guided by a competition between solvent and lipids for interacting with the periplasmic loops. A similar observation has recently been pointed out by Meyer *et al.*,[36] who observed large conformational changes in this region when the *E. coli* MscL is placed in curved lipid membrane.

Principal component analysis and normal mode

In this study we performed a direct comparison of the normal modes computed with the coarse-grained Tirion's potential,[67] and principal modes describing the fluctuations of a MD trajectory computed with an all-atom force field. Despite the large differences in the explored systems (force-field, environment, harmonic vs. anharmonic motion analysis, etc), similarities exist between the results of the two approaches. Comparison of DMPE eigenvectors and NMA-modes indicates that the modification of membrane thickness simply accelerates the conformational changes along what we can consider as the "natural" directions of the conformational changes involved in the mechanics of the channel. It provides also additional evidence about the relevance of the normal mode analysis with a crude elastic model.

CONCLUSIONS

This study has permitted us to give new insights in the adaptation of the MscL to membrane thickness changes. We thus provide a detailed structural description of a putative intermediate along the channel gating, and bring new clues about the role of the periplasmic loops that may act as springs partly controlling the mechanical pathway. We also confirm that tilting is a major response of a transmembrane channel to membrane thickness change. Moreover, this work reinforce the observation we previously discussed, namely, that transmembrane helices are flexible, able to deform without any significant conformational cost. For a given helix, the major deforma-

tions are concerned with local kinks while the secondary structure is roughly maintained on both sides of the kink region. In addition, the kink is mainly located in the region close to the constricted region of the pore as we already observed with NMA analysis.

Overall, from a theoretical point of view, this study conducted with an all-atom force field in a complex environment strengthens the results obtained with a normal mode analysis. It confirms the relevance of an approach based on Tirion's potential.

ACKNOWLEDGMENTS

The authors thank Dr. Patrick Fuchs and Dr. Alexandre De Brevern for their fruitful comments. Gaelle Debret benefits from a fellowship from the French government (MENRT).

REFERENCES

1. Ajouz B, Berrier C, Garrigues A, Besnard M, Ghazi A. Release of thioredoxin via the mechanosensitive channel MscL during osmotic downshock of *Escherichia coli* cells. J Biol Chem 1998;273:26670–26674.
2. Ewis HE, Lu CD. Osmotic shock: a mechanosensitive channel blocker can prevent release of cytoplasmic but not periplasmic proteins. FEMS Microbiol Lett 2005;253:295–301.
3. Blount P, Sukharev S, Kung C. A mechanosensitive channel protein and its gene in *E. coli*. Gravit Space Biol Bull 1997;10:43–47.
4. Blount P, Sukharev SI, Schroeder MJ, Nagle SK, Kung C. Single residue substitutions that change the gating properties of a mechanosensitive channel in *Escherichia coli*. Proc Natl Acad Sci USA 1996;93:11652–11657.
5. Blount P, Schroeder MJ, Kung C. Mutations in a bacterial mechanosensitive channel change the cellular response to osmotic stress. J Biol Chem 1997;272:32150–32157.
6. Cruickshank CC, Minchin RF, Le Dain AC, Martinac B. Estimation of the pore size of the large-conductance mechanosensitive ion channel of *Escherichia coli*. Biophys J 1997;73:1925–1931.
7. Hase CC, Le Dain AC, Martinac B. Molecular dissection of the large mechanosensitive ion channel (MscL) of *E. coli*: mutants with altered channel gating and pressure sensitivity. J Membr Biol 1997;157:17–25.
8. Hase CC, Minchin RF, Kloda A, Martinac B. Cross-linking studies and membrane localization and assembly of radiolabelled large mechanosensitive ion channel (MscL) of *Escherichia coli*. Biochem Biophys Res Commun 1997;232:777–782.
9. Ou X, Blount P, Hoffman RJ, Kung C. One face of a transmembrane helix is crucial in mechanosensitive channel gating. Proc Natl Acad Sci USA 1998;95:11471–11475.
10. Sukharev SI, Sigurdson WJ, Kung C, Sachs F. Energetic and spatial parameters for gating of the bacterial large conductance mechanosensitive channel, MscL. J Gen Physiol 1999;113:525–540.
11. Yoshimura K, Batiza A, Schroeder M, Blount P, Kung C. Hydrophilicity of a single residue within MscL correlates with increased channel mechanosensitivity. Biophys J 1999;77:1960–1972.
12. Ajouz B, Berrier C, Besnard M, Martinac B, Ghazi A. Contributions of the different extramembranous domains of the mechanosensitive ion channel MscL to its response to membrane tension. J Biol Chem 2000;275:1015–1022.
13. Perozo E, Kloda A, Cortes DM, Martinac B. Site-directed spin-labeling analysis of reconstituted Mscl in the closed state. J Gen Physiol 2001;118:193–206.
14. Yoshimura K, Batiza A, Kung C. Chemically charging the pore constriction opens the mechanosensitive channel MscL. Biophys J 2001;80:2198–2206.
15. Levin G, Blount P. Cysteine scanning of MscL transmembrane domains reveals residues critical for mechanosensitive channel gating. Biophys J 2004;86:2862–2870.
16. Li Y, Wray R, Blount P. Intragenic suppression of gain-of-function mutations in the *Escherichia coli* mechanosensitive channel, MscL. Mol Microbiol 2004;53:485–495.
17. Park KH, Berrier C, Martinac B, Ghazi A. Purification and functional reconstitution of N- and C-halves of the MscL channel. Biophys J 2004;86:2129–2136.
18. Yoshimura K, Nomura T, Sokabe M. Loss-of-function mutations at the rim of the funnel of mechanosensitive channel MscL. Biophys J 2004;86:2113–2120.
19. Chiang CS, Shirinian L, Sukharev S. Capping transmembrane helices of MscL with aromatic residues changes channel response to membrane stretch. Biochemistry 2005;44:12589–12597.
20. Corry B, Rigby P, Liu ZW, Martinac B. Conformational changes involved in MscL channel gating measured using FRET spectroscopy. Biophys J 2005;89:L49–L51.
21. Nguyen T, Clare B, Guo W, Martinac B. The effects of parabens on the mechanosensitive channels of *E. coli*. Eur Biophys J 2005;34:389–395.
22. Tsai IJ, Liu ZW, Rayment J, Norman C, McKinley A, Martinac B. The role of the periplasmic loop residue glutamine 65 for MscL mechanosensitivity. Eur Biophys J 2005;34:403–412.
23. Kloda A, Ghazi A, Martinac B. C-terminal charged cluster of MscL. RKKEE, functions as a pH sensor. Biophys J 2006;90:1992–1998.
24. Bartlett JL, Li Y, Blount P. Mechanosensitive channel gating transitions resolved by functional changes upon pore modification. Biophys J 2006;91:3684–3691.
25. van den Bogaart G, Krasnikov V, Poolman B. Dual-color fluorescence-burst analysis to probe protein efflux through the mechanosensitive channel MscL. Biophys J 2007;92:1233–1240.
26. Chang G, Spencer RH, Lee AT, Barclay MT, Rees DC. Structure of the MscL homolog from *Mycobacterium tuberculosis*: a gated mechanosensitive ion channel. Science 1998;282:2220–2226.
27. Steinbacher S, Bass R, Strop P, Rees DC. Structures of the prokaryotic mechanosensitive channels MscL and MscS. Curr Top Membr 2007;58:1–24.
28. Perozo E, Cortes DM, Sompornpisut P, Kloda A, Martinac B. Open channel structure of MscL and the gating mechanism of mechanosensitive channels. Nature 2002;418:942–948.
29. Sukharev S, Durell SR, Guy HR. Structural models of the MscL gating mechanism. Biophys J 2001;81:917–936.
30. Sukharev S, Betanzos M, Chiang CS, Guy HR. The gating mechanism of the large mechanosensitive channel MscL. Nature 2001;409:720–724.
31. Leach AR. Molecular Modelling: Principles and Applications. Harlow, UK: Prentice Hall; 2001.
32. Gullingsrud J, Schulten K. Lipid bilayer pressure profiles and mechanosensitive channel gating. Biophys J 2004;86:3496–3509.
33. Gullingsrud J, Kosztin D, Schulten K. Structural determinants of MscL gating studied by molecular dynamics simulations. Biophys J 2001;80:2074–2081.
34. Gullingsrud J, Schulten K. Gating of MscL studied by steered molecular dynamics. Biophys J 2003;85:2087–2099.
35. Colombo G, Marrink SJ, Mark AE. Simulation of MscL gating in a bilayer under stress. Biophys J 2003;84:2331–2337.
36. Meyer GR, Gullingsrud J, Schulten K, Martinac B. Molecular dynamics study of MscL interactions with a curved lipid bilayer. Biophys J 2006;91:1630–1637.
37. Elmore DE, Dougherty DA. Investigating lipid composition effects on the mechanosensitive channel of large conductance (MscL) using molecular dynamics simulations. Biophys J 2003;85:1512–1524.

38. Perozo E, Kloda A, Cortes DM, Martinac B. Physical principles underlying the transduction of bilayer deformation forces during mechanosensitive channel gating. Nat Struct Biol 2002;9:696–703.
39. Moe PC, Levin G, Blount P. Correlating a protein structure with function of a bacterial mechanosensitive channel. J Biol Chem 2000;275:31121–31127.
40. Valadie H, Lacapcre JJ, Sanejouand YH, Etchebest C. Dynamical properties of the MscL of *Escherichia coli*: a normal mode analysis. J Mol Biol 2003;332:657–674.
41. Tama F, Sanejouand YH. Conformational change of proteins arising from normal mode calculations. Protein Eng 2001;14:1–6.
42. Krebs WG, Alexandrov V, Wilson CA, Echols N, Yu H, Gerstein M. Normal mode analysis of macromolecular motions in a database framework: developing mode concentration as a useful classifying statistic. Proteins 2002;48:682–695.
43. Miyashita O, Onuchic JN, Wolynes PG. Nonlinear elasticity, proteinquakes, and the energy landscapes of functional transitions in proteins. Proc Natl Acad Sci USA 2003;100:12570–12575.
44. Tai K, Shen T, Borjesson U, Philippopoulos M, McCammon JA. Analysis of a 10-ns molecular dynamics simulation of mouse acetylcholinesterase. Biophys J 2001;81:715–724.
45. Snow C, Qi G, Hayward S. Essential dynamics sampling study of adenylate kinase: comparison to citrate synthase and implication for the hinge and shear mechanisms of domain motions. Proteins 2007;67:325–337.
46. Spiwok V, Lipovova P, Kralova B. Metadynamics in essential coordinates: free energy simulation of conformational changes. J Phys Chem B 2007;111:3073–3076.
47. Morein S, Andersson A, Rilfors L, Lindblom G. Wild-type *Escherichia coli* cells regulate the membrane lipid composition in a "window" between gel and non-lamellar structures. J Biol Chem 1996; 271:6801–6809.
48. Tieleman DP, Berendsen HJ. A molecular dynamics study of the pores formed by *Escherichia coli* OmpF porin in a fully hydrated palmitoyloleoylphosphatidylcholine bilayer. Biophys J 1998;74:2786–2801.
49. Blount P, Sukharev SI, Moe PC, Nagle SK, Kung C. Towards an understanding of the structural and functional properties of MscL, a mechanosensitive channel in bacteria. Biol Cell 1996;87:1–8.
50. Lindahl E, Edholm O. Molecular dynamics simulation of NMR relaxation rates and slow dynamics in lipid bilayer. J Chem Phys 2001;115:4938–4950.
51. Berendsen HJ, van der Spoel D, van Drunen R. GROMACS: a message-passing parallel molecular dynamics implementation. Comput Phys Commun 1995;91:43–56.
52. Berger O, Edholm O, Jahnig F. Molecular dynamics simulations of a fluid bilayer of dipalmitoylphosphatidylcholine at full hydration, constant pressure, and constant temperature. Biophys J 1997;72: 2002–2013.
53. Hess B, Bekker H, Berendsen HJC, Fraaije JGEM. LINCS: a linear constraint solver for molecular simulations. J Comput Chem 1997; 18:1463–1472.
54. Berendsen HJC, Postma JPM, van Gunsteren WF, Di Nola A, Haak JR. Molecular dynamics with coupling to an external bath. J Chem Phys 1984;81:3684–3690.
55. Smart OS, Goodfellow JM, Wallace BA. The pore dimensions of gramicidin A. Biophys J 1993;65:2455–2460.
56. Humphrey W, Dalke A, Schulten K. VMD: visual molecular dynamics. J Mol Graph 1996;14:33–38, 27–38.
57. Hess B. Convergence of sampling in protein simulations. Phys Rev E Stat Nonlin Soft Matter Phys 2002;65(3, Part 1):031910.
58. Marques O, Sanejouand YH. Hinge-bending motion in citrate synthase arising from normal mode calculations. Proteins 1995;23:557–560.
59. Bruschweiler R. Collective protein dynamics and nuclear spin relaxation. J Chem Phys 1995;102:3396–3403.
60. Mao G, Chen D, Handa H, Dong W, Kurth DG, Mohwald H. Deposition and aggregation of aspirin molecules on a phospholipid bilayer pattern. Langmuir 2005;21:578–585.
61. Helm CA, Tippmann-Krayer P, Mohwald H, Als-Nielsen J, Kjaer K. Phases of phosphatidyl ethanolamine monolayers studied by synchrotron X-ray scattering. Biophys J 1991;60:1457–1476.
62. Rand RP, Parsegian VA. Hydratation forces between phospholipid bilayers. Biochem Biophys Acta 1989;988:351–376.
63. Elmore DE, Dougherty DA. Molecular dynamics simulations of wild-type and mutant forms of the *Mycobacterium tuberculosis* MscL channel. Biophys J 2001;81:1345–1359.
64. Capener CE, Shrivastava IH, Ranatunga KM, Forrest LR, Smith GR, Sansom MS. Homology modeling and molecular dynamics simulation studies of an inward rectifier potassium channel. Biophys J 2000;78:2929–2942.
65. Sotomayor M, Schulten K. Molecular dynamics study of gating in the mechanosensitive channel of small conductance MscS. Biophys J 2004;87:3050–3065.
66. Park SH, Opella SJ. Tilt angle of a trans-membrane helix is determined by hydrophobic mismatch. J Mol Biol 2005;350:310–318.
67. Tirion M. Large amplitude elastic motions in proteins from a single-parameter, atomic analysis. Phys Rev Lett 1996;77:1905–1908.